

PACS 72.20.J, 78.55, 78.60

# Evaluation of the efficiency of interband radiative recombination in high quality Si

A.V. Sachenko, Yu.V. Kryuchenko

Institute of Semiconductor Physics, NAS of Ukraine,  
45, prospect Nauki, 03028 Kiev, Ukraine

**Abstract.** It is shown theoretically that quantum efficiency of interband radiation in highly purified silicon with low concentration of deep impurities and defects can exceed 10% at room temperatures in the case of negligibly small surface recombination. Dependencies of quantum efficiency on intensity and wavelength of exciting monochromatic light, surface recombination rate and thickness of silicon plate are discussed.

**Keywords:** interband radiative recombination in silicon, high excitation, quantum efficiency.

Paper received 19.10.99; revised manuscript received 14.12.99; accepted for publication 17.12.99.

## 1. Introduction

Since silicon is indirect gap semiconductor it is characterized by substantially lower probability of interband radiative recombination than direct gap materials. However, unlike many other materials Si can be very effectively cleaned from different impurities which are responsible for existence of recombination levels. For example, [1-4] data give evidence that characteristic time of Shockley-Reed-Hall nonradiative recombination in silicon can be as high as  $10^{-2}$  s, which is the record large one among all semiconductor materials. At the specified conditions and sufficiently high excitation level the probability of radiative interband recombination can exceed the probability of nonradiative Shockley-Reed-Hall recombination. In this case, though limited by Auger recombination, quantum efficiency of radiative interband recombination has to increase substantially. In the present work this problem is analyzed theoretically and some estimates are made of both quantum efficiency of interband radiative recombination and its dependence on excitation level in highly purified silicon at room temperatures.

## 2. Problem formulation

According to paper [5], at high excitation levels not only quadratic recombination due to radiative interband transitions occurs in Si, but Auger recombination due to traps as well. The last one is also quadratic over carrier concentration and depends linearly on impurity concentration. Most likely, it is just the Auger recombination that gives dominant contribution in works [6, 7] where investigation of recombi-

nation processes in Si at laser excitation levels has been made. This recombination is ignored in the present work because the unique case of extremely small concentrations of deep impurities is considered here.

Up to date the value  $2 \cdot 10^{-15} \text{ cm}^3 \cdot \text{c}^{-1}$  has been used for the constant  $A_i$  of interband radiative recombination in silicon at  $T = 300 \text{ K}$  [8,9]. However, in paper [10] more precise value  $A_i \cong 1.5 \cdot 10^{-15} \text{ cm}^3 \cdot \text{c}^{-1}$  was obtained using data of [11] on the absorption coefficient in the region of absorption edge of high quality Si. This  $A_i$  value was determined with the standard detailed balancing method. Within the framework of this method the flux of radiative recombination is equal to the optical electron-hole generation flux caused by the absorption of equilibrium photons in Si. We have used this last  $A_i$  value in calculations for the present work.

To find concentration of excess electron-hole pairs at an arbitrary level of monochromatic excitation one has to solve the following ambipolar diffusion equation:

$$\frac{\partial}{\partial x} \left( D(x) \frac{\partial \Delta n(x)}{\partial x} \right) - \frac{\Delta n(x)}{\tau(x)} + \alpha(\lambda) I_0 (1 - r_s(\lambda)) \times \exp(-\alpha(\lambda)x) = 0 \quad (1)$$

with the boundary conditions

$$j_n \Big|_{x=0,d} = -D(x) \frac{\partial \Delta n(x)}{\partial x} \Big|_{x=0,d} = \mp s_x \Delta n(x) \Big|_{x=0,d} \quad (2)$$

Upper sign in the right hand side of Eq. (2) has to be taken for  $x = 0$  and the lower one for  $x = d$ ,  $D(x)$  is the ambipolar diffusion coefficient,  $\Delta n(x)$  the concentration of excess electron-hole pairs generated by an external excitation,

$$\frac{1}{\tau(x)} = \frac{1}{\tau_r(x)} + A_i(p_0 + \Delta n(x)) + C_p(p_0 + \Delta n(x))^2 + C_n \Delta n(x)(p_0 + \Delta n(x)) \quad (3)$$

is the probability of bulk carrier recombination,  $\tau_r(x)$  is Shockley-Reed-Hall life time,  $C_p$  and  $C_n$  are the constants of interband Auger recombination for holes and electrons respectively,  $x$  is the distance from the front illuminated surface of the sample,  $p_0$  is equilibrium hole concentration in  $p$ -type semiconductor,  $a(\lambda)$  and  $r_s(\lambda)$  are the absorption and reflection coefficients for the monochromatic exciting light with the wave length  $\lambda$ ,  $I_0$  is the intensity of exciting light,  $d$  is the sample thickness,  $j_n(x=0,d)$  is the carrier flux at the sample boundaries,  $s_{0(d)}$  is the surface recombination rate at the front and rear surfaces of the sample.

In a general case  $D(x)$ ,  $\tau_r(x)$  and  $s_{0(d)}$  are the functions of excitation level. Ambipolar diffusion coefficient is given by the following formula:

$$D(x) = \frac{D_n(x)D_p(x)(p_0 + n_0 + 2\Delta n(x))}{D_n(x)(p_0 + \Delta n(x)) + D_p(x)(n_0 + \Delta n(x))} \quad (4)$$

It depends on excitation level both directly through the carrier concentration  $\Delta n(x)$  and indirectly through the diffusion coefficients of electrons  $D_n(x)$  and holes  $D_p(x)$  which can change their values at high excitation levels due to increased electron-hole scattering [12,13]. According to [12], if the temperature is high enough the electron-hole scattering in lightly doped Si has noticeable effect only in the region of  $\Delta n(x)/p_0 \gg 1$ . At extremely high excitation levels this scattering is responsible for disappearance of a difference between electron and hole diffusion coefficients and their saturation. Estimated diffusion coefficients vary only slightly with excitation level in the region of interest (changes in  $D$  do not exceed two times). Therefore, the influence of  $D(x)$  variations on the considered effect is very weak comparing to the influence of strong changes (orders of magnitude) in  $t(x)$ . Moreover, in the region of  $L_d(x) = \sqrt{D(x)\tau(x)} \gg d$  the effect is completely insensitive to a specific  $D(x)$  value. For this reason we confine here our consideration to the case of  $D(x)=const$ .

In accordance with Shockley-Reed-Hall statistics the bulk carrier lifetime  $\tau_r(x)$  for the process of nonradiative carrier recombination through the recombination centers is expressed by the following formula:

$$\tau_r(x) = \frac{\tau_p(n_0 + \Delta n(x) + n_i \exp(\epsilon_r))}{n_0 + p_0 + \Delta n(x)} + \frac{\tau_n(p_0 + \Delta n(x) + n_i \exp(-\epsilon_r))}{n_0 + p_0 + \Delta n(x)} \quad (5)$$

where  $\tau_p = (s_p V_T N_r)^{-1}$ ,  $\tau_n = (s_n V_T N_r)^{-1}$ ,  $\sigma_p$  and  $\sigma_n$  are the cross sections of hole and electron trapping by a recombination center,  $V_T$  the thermal velocity,  $N_r$  the concentration of recombination centers,  $\epsilon_r = (E_r - E_i)/kT$  the dimensionless recombination center energy measured from the center of a bandgap,  $n_0$  and  $n_i$  are the equilibrium electron concentration and that of electrons in intrinsic semiconductor respectively.

Two cases of surface recombination are considered:

$$s_{0(d)} = const \quad (6)$$

$$s_{0(d)} = s \times \left( 1 + \frac{\Delta n(x)}{p_0} \right)_{x=0,d} \quad (7)$$

The first case is realized when  $\Delta n(x) \gg p_0$  and a depletive initial band bending at surfaces of a semiconductor plate takes place. The second case expressed by Eq. (7) is realized when the following requirements are met: a) concentration of excess electron-hole pairs inside a semiconductor is much less than equilibrium surface electron concentration (if inverse conductivity at surfaces takes place); b) concentration of surface states is much less than surface concentration of excess electrons (if inverse conductivity takes place) or excess holes (if accumulation occurs at the surfaces).

Quantum efficiency of radiative interband recombination can be found using the following formula:

$$\eta = \frac{\int_0^d A_i \Delta n(x)(p_0 + \Delta n(x)) \, dx}{\int_0^d \frac{\Delta n(x)}{\tau(x)} \, dx + s_0 \Delta n(0) + s_d \Delta n(d)} \quad (8)$$

Of course, previously it is necessary to solve Eq. (1) taking into account Eqs. (2)-(7) and find  $\Delta n(x)$  function.

### 3. Results and discussion

Eq.(1) has been solved numerically using following specific values of parameters:  $C_p = 10^{-31}$  and  $C_n = 2.8 \cdot 10^{-31} \text{ cm}^6 \cdot \text{s}^{-1}$  [14],  $D = 18 \text{ cm}^2 \cdot \text{s}^{-1}$ ,  $p_0 = 10^{14} \text{ cm}^{-3}$ . For Shockley-Reed-Hall lifetime the value  $t_r = 20 \text{ ms}$  was used in all considered cases except those illustrated in Fig. 3(b, c). Intensity  $I = I_0(1-r_s)$  of the exciting light passed through the front surface into semiconductor has been varied from  $10^{14}$  to  $10^{22} \text{ cm}^{-2} \cdot \text{s}^{-1}$ . Only the case of equal surface recombination rates at the front and rear surfaces has been considered when using Eq. (6). Spectral dependency of absorption coefficient  $\alpha(\lambda)$  was taken from paper [15].

Fig. 1 illustrates dependencies of the concentration of excess electron-hole pairs  $\Delta n$  on the distance  $x$  from the front surface for the case of plate thickness  $d = 100 \text{ nm}$ . Curves are built at different values of the excitation intensity  $I$ . As one can see from this figure the dependencies  $\Delta n(x)$  become linear with decrease in intensity  $I$ , and at  $I < 10^{20} \text{ cm}^{-2} \cdot \text{s}^{-1}$   $\Delta n(d)$  differs from  $\Delta n(0)$  no more than by 10 % (it means that in this case local diffusion length).

Dependencies of the excess carrier concentration at  $x = 0$  on the intensity  $I$  are given in Fig.2. Steep parts of curves at relatively low intensities correspond to linear increase in  $\Delta n(0)$  with  $I$ . At  $s_{0(d)} \neq 0$  such behavior is provided by the dominant contribution of the first  $\tau_r$ -term in Eq. (3), i.e. it is connected with Shockley-Reed-Hall recombination. At  $s_{0(d)} \approx 0$  the surface recombination is responsible for steep slopes of curves. In a narrow transition region of intensities quadratic (radiative) and cubic (Auger) recombination begin to

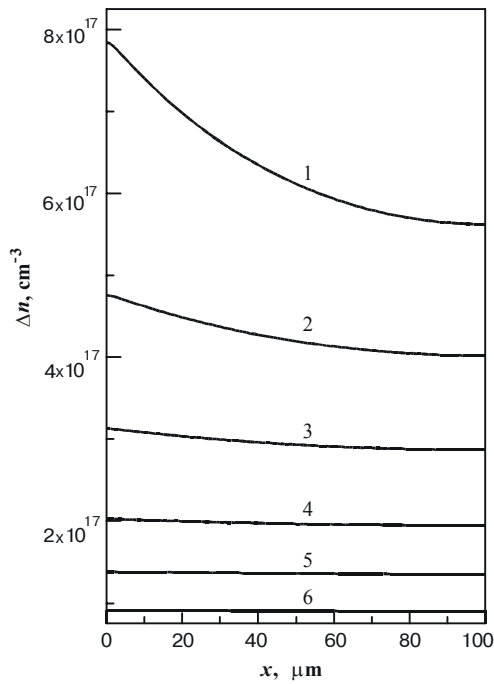


Fig. 1. Concentration of excess electrons in Si plate as function of distance  $x$  from the front surface. Intensities of exciting light  $I$ ,  $\text{cm}^{-2}\cdot\text{s}^{-1}$ :  $10^{21}$  (curve 1),  $3\cdot 10^{20}$  (2),  $10^{20}$  (3),  $3\cdot 10^{19}$  (4),  $10^{19}$  (5) and  $3\cdot 10^{18}$  (6). Parameters used:  $\lambda = 0.5 \mu\text{m}$ ,  $d = 100 \mu\text{m}$ ,  $s_{0(d)} = 0$ .

play predominant role thus giving  $\Delta n(0) \sim I^{1/3}$  low at higher intensities. As one can see from Fig. 2 the more is the value of  $s_{0(d)}$  the higher intensities  $I$  are required to reach the transition region.

Fig. 3(a) illustrates the dependencies of quantum efficiency of interband radiation on the intensity  $I$  of exciting

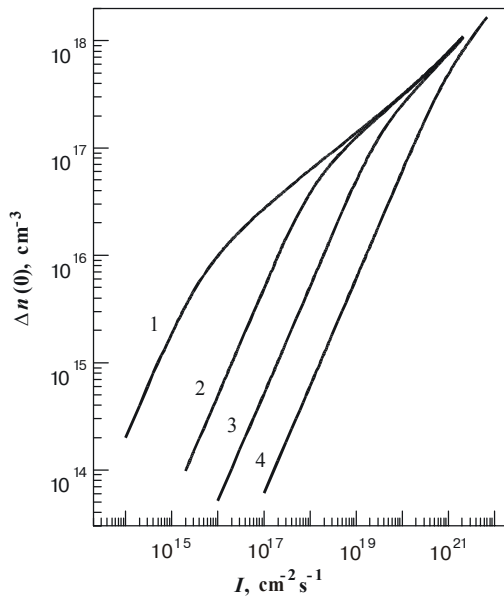


Fig. 2. Concentration of excess electrons at the front surface ( $x = 0$ ) of Si plate as function of excitation intensity  $I$ . Surface recombination rates  $s_{0(d)}$ ,  $\text{cm}\cdot\text{s}^{-1}$ : 0 (curve 1), 10 (2), 100 (3) and 1000 (4). Parameters used:  $\lambda = 0.5 \mu\text{m}$ ,  $d = 100 \mu\text{m}$ .

light passed through the front surface into the crystal. Surface recombination rate served as a curve parameter. Curves (1)–(5) correspond to the case of Eq. (6) with surface recombination rate independent of excitation level, while curves (6)–(8) to the case of Eq. (7). As one can see from this figure the more is surface recombination rate  $s_{0(d)}$  the less is quantum efficiency  $\eta$ . The region of  $\eta$  increase with the intensity corresponds to the dominant contribution of bulk Shockley-Reed-Hall recombination (curves 1, 2 and 6) or surface recombination (curves 3, 4, 5, 7 and 8) while the region of  $\eta$  decrease to the dominant role of Auger recombination. The more is  $s_{0(d)}$  value the more is the displacement of the maximum in  $\eta(I)$  dependencies into the region of high intensities. For the case of negligibly small surface recombination the maximal calculated quantum efficiency reaches the value of about 15% which is several orders of magnitude larger than observed earlier in experiments. It is caused mainly by the fact that the bulk Shockley-Reed-Hall lifetime in conventional material is 1–10  $\mu\text{s}$  which is 3–4 orders of magnitude lower than in highly purified silicon with very low concentration of deep impurities and defects.

It is seen also from this figure that in the case of  $s(\Delta n)$  functional dependency (Eq. (7)) the quantum efficiency decreases substantially even if at low intensities the surface recombination rate is lower than  $1 \text{ cm}\cdot\text{s}^{-1}$ . In the region  $\Delta n \gg p_0$  this functional dependency simulates quadratic recombination. Therefore in a common case a problem arises of discrimination between this mechanism of recombination and the bulk Auger recombination involving impurities.

In Fig. 3(b) the dependencies  $\eta(I)$  at different values of Shockley-Reed-Hall lifetime  $\tau_r$  are shown for the case of zero surface recombination rate. It is seen that decrease in  $\tau_r$  leads to decrease in quantum efficiency of radiative recombination with displacement of maximal  $\eta$  values in the region of high intensities (curve 7). Nevertheless, even with  $\tau_r$  decrease by three orders of magnitude quantum efficiency decreases only by one order of magnitude thus staying markedly large.

Fig. 3(c) illustrates the influence of functional changes in Shockley-Reed-Hall lifetime (see Eq. (5)) on quantum efficiency at intermediate excitation levels in the case of negligibly small surface recombination. As one can see from this figure the indicated influence takes place only at relatively moderate excitation levels and practically doesn't change  $\eta$  in the region of its maximum. Moreover, as it follows from above analysis, in  $p$ -Si material with a bulk recombination level of the donor type near the center of bandgap the case of  $\tau_r(\Delta n(x)) = \text{const}$  is realized and thus no influence has to be observed. An analogous situation takes place in a semiconductor of  $n$ -type if the recombination level is of acceptor type.

In Fig. 4 spectral dependencies of quantum efficiency are shown for the excitation intensity  $I_0 = 3\cdot 10^{19} \text{ cm}^{-2}\cdot\text{s}^{-1}$ . Surface recombination rate served as curve parameter. It is seen from this figure that flattening of dependencies occurs in the region of short wave lengths. The larger is the value of surface recombination rate the lower is quantum efficiency. Taking into account a decrease in excess concentration  $\Delta n(x)$  near absorption edge due to incomplete absorption of long-wavelength light passed into the crystal, it becomes appar-

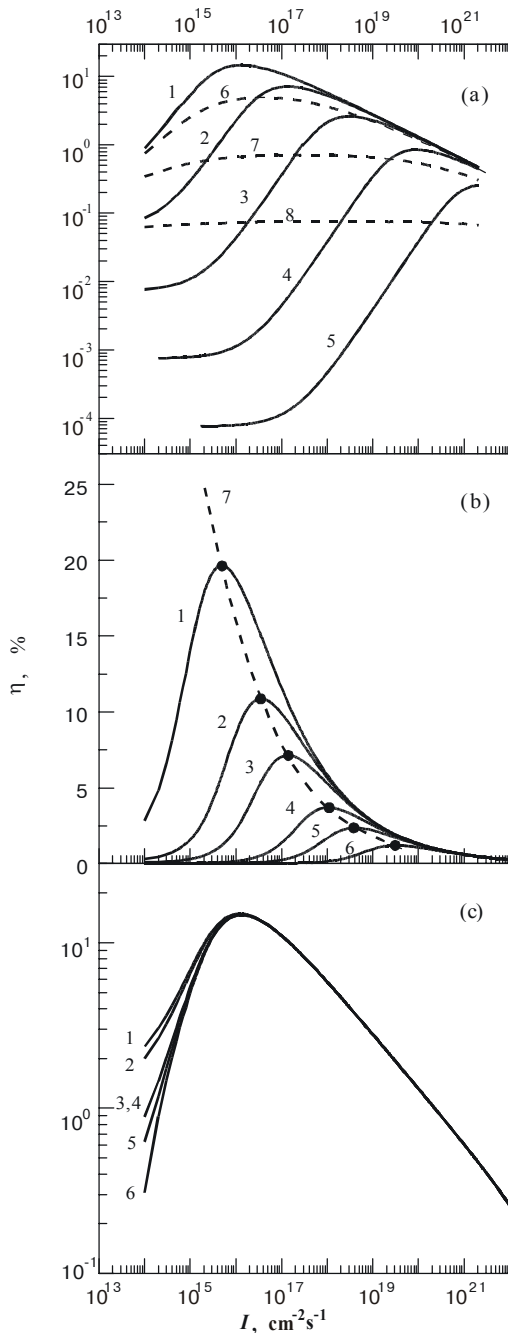


Fig.3. Quantum efficiency of interband radiation as function of excitation intensity  $I$  for the case of  $\lambda = 0.5 \text{ mm}$  and  $d = 100 \text{ }\mu\text{m}$ .  
 (a) The intensity-independent surface recombination rates  $s_{0(d)}$ ,  $\text{cm}^{-2}\text{s}^{-1}$ : 0 (curve 1), 1 (2), 10 (3), 100 (4) and 1000 (5). Coefficient  $s$  in expression (7) for the case of functional dependence  $s_{0(d)}(I)$ ,  $\text{cm}^{-2}\text{s}^{-1}$ : 0.01 (curve 6), 0.1 (7) and 1 (8). Shockley-Reed-Hall life time  $t_r = 20 \text{ ms}$ .  
 (b) The intensity-independent Shockley-Reed-Hall life times  $t_r$ , ms: 40 (curve 1), 10 (2), 4 (3), 1 (4), 0.4 (5) and 0.1 (6). Surface recombination rate  $s_{0(d)} = 0$ .  
 (c) The intensity-dependent Shockley-Reed-Hall life times  $t_r$  according to Eq.(5):  $\tau_p = 0.1 \text{ ms}$ ,  $\tau_n = 20 \text{ ms}$ ,  $E_r - E_i = 0.4 \text{ eV}$  (curve 1);  $\tau_p = 20 \text{ ms}$ ,  $\tau_n = 0.1 \text{ ms}$ ,  $E_r - E_i = -0.4 \text{ eV}$  (curve 2);  $\tau_p = 0.1 \text{ ms}$ ,  $\tau_n = 20 \text{ ms}$ ,  $E_r - E_i = 0.2 \text{ eV}$  (curve 3);  $\tau_r = \text{const} = 20 \text{ ms}$  (curve 4);  $\tau_p = 10 \text{ ms}$ ,  $\tau_n = 10 \text{ ms}$ ,  $E_r - E_i = 0$  (curve 5);  $\tau_p = 20 \text{ ms}$ ,  $\tau_n = 0.1 \text{ ms}$ ,  $E_r - E_i = -0.2 \text{ eV}$  (curve 6). Surface recombination rate  $s_{0(d)} = 0$ .

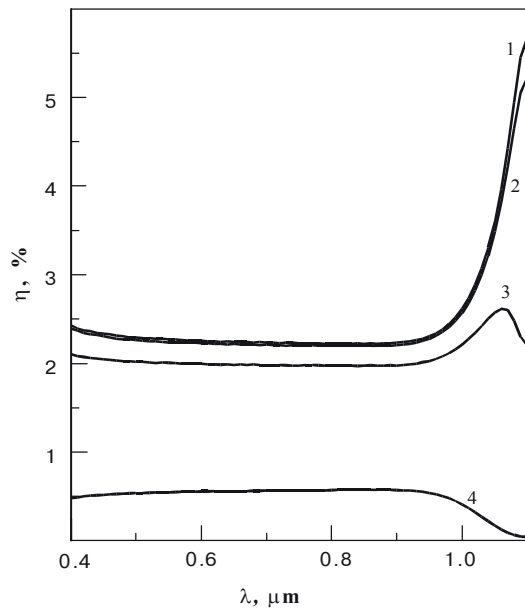


Fig.4. Spectral dependencies of interband radiation quantum efficiency. Surface recombination rates  $s_{0(d)}$ ,  $\text{cm}^{-2}\text{s}^{-1}$ : 0 (curve 1), 1 (2), 10 (3) and 100 (4). Parameters used:  $I_0 = 3 \cdot 10^{19} \text{ cm}^{-2} \text{ s}^{-1}$ ,  $d = 100 \text{ }\mu\text{m}$ .

ent that spectral dependencies of quantum efficiency correlate with  $\eta(I)$  dependencies shown in Fig. 3(a).

Quantum efficiency dependencies on thickness  $d$  of Si plate are shown in Fig. 5. In general, expression (8) for  $\eta$  is valid only in the case if zero reabsorption of interband radiation take place. Obviously, for a plate of large thickness the reabsorption lowers quantum efficiency, and therefore it is necessary to take into account this effect to obtain more realistic  $\eta$  values. We accounted for reabsorption by simply multiplying expression (8) into  $1/(1+a^*d)$  factor, where  $a^*$  is the experimental value of absorption coefficient at Si bandgap energy. According to [11] this value is  $1.5 \text{ cm}^{-1}$ . It

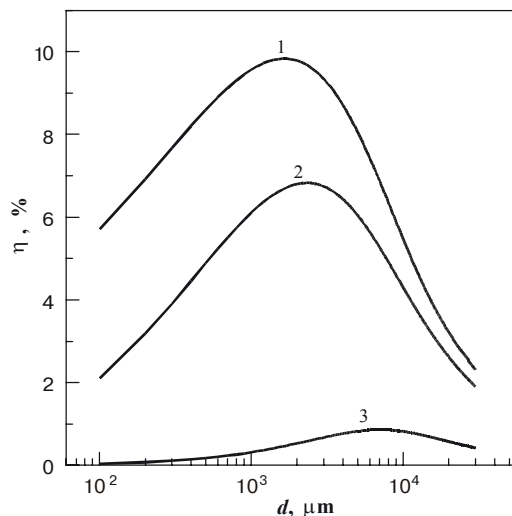


Fig.5. Quantum efficiency of interband radiation as a function of Si plate thickness  $d$ . Surface recombination rates  $s_{0(d)}$ ,  $\text{cm}^{-2}\text{s}^{-1}$ : 0 (curve 1), 10 (2), 100 (3) and 1000 (4). Parameters used:  $I = 10^{18} \text{ cm}^{-2}\text{s}^{-1}$ ,  $d = 100 \text{ }\mu\text{m}$ .

is seen from this figure that at small thicknesses quantum efficiency increases with  $d$  due to relative enlargement of bulk recombination effect at this stage. Then  $\eta$  passes through the maximum and begin to decrease at relatively large thicknesses due to the increased role of reabsorption effect. Remarkably large difference between  $\eta$  values in the region of large thicknesses for different  $s$  can be explained by the fact that the dependencies in this figure correspond to a specific case of highly absorbed excitation. Under weak absorption this difference will be substantially lower.

Finally, to evaluate the influence of many-particle effects on the obtained results, quantum efficiency of radiative recombination in  $p$ -Si has been calculated taking into account both electron-hole interactions (exciton effects) and electron-electron interactions which can correct radiative interband and nonradiative Auger recombination [16,17]. These effects are responsible for the increase in both radiative recombination probability (larger  $A_i$  constant) and Auger parameter for electrons. Moreover, the latter becomes dependent on the excess carrier concentration. At such conditions experimentally determined  $A_i$  value for Si at  $T=300$  K is  $3 \cdot 10^{-15}$  cm<sup>3</sup>/s [2], while theory gives higher value  $A_i \approx 6 \cdot 10^{-15}$  cm<sup>3</sup>/s [16]. For  $\Delta n$  in the region  $10^{15} \div 10^{19}$  cm<sup>-3</sup> Auger recombination parameter for electrons in accordance

with experimental data of [17] can be approximated by the following formula:

$$C_n = \left( 2.8 \cdot 10^{-31} + \frac{2.5 \cdot 10^{-22}}{\sqrt{\Delta n}} \right) \text{cm}^6 / \text{s} \quad (9)$$

Fig. 6 illustrates the corresponding dependencies of quantum efficiency of radiative interband recombination on excitation light intensity for the case of  $s_{0(d)} = 0$ . It is clear from the figure that principal consequences of the consideration without many-particle effects are valid, although many-particle effects somewhat lead to changes in  $\eta$  value.

## Conclusions

In the present work it is shown theoretically that quantum efficiency of interband radiation in highly purified silicon under room temperature may be as much as 20%. On the one hand, it is caused by uniquely large values of bulk Shockley-Reed-Hall lifetime and, on the other hand, by negligibly weak Auger recombination with participation of deep impurities in such Si crystals. It is shown that in this case surface recombination can be responsible for substantial decrease in quantum efficiency. Most likely the record quantum efficiency values can be obtained in Si-SiO<sub>2</sub> structures with low density of surface states.

## References

1. E. Yablonovitch and T. Gmitter. Auger recombination in silicon at low carrier densities // *Appl. Phys. Lett.*, **49**, pp.587-589 (1986)
2. S.K. Pang and A. Rohatgi. Record high recombination lifetime in oxidized magnetic Czochralski silicon // *Appl. Phys. Lett.*, **59**, pp.195-197 (1991)
3. R. Hacker and A. Hangleiter // *J. Appl. Phys.*, **75**, pp.7570- (1994)
4. J. Linnros. Carrier lifetime measurements using free carrier absorption transients. I. Principle and injection dependence // *J. Appl. Phys.*, **84**, pp.275-283 (1998)
5. W. Gerlach, H. Schlagenotto and H. Maeder. On the radiative recombination rate in silicon // *Phys. Stat. Sol.*, **A13**, pp.277-283 (1972)
6. V.A. Zuev, V.G. Litovchenko, K.D. Glinchuk, et all. Processy rekombinazii nositelei toka na poverkhnosti Ge i Si pri lazernykh vzbuzhdeniyakh (Processes of carrier recombination at Ge and Si surfaces under laser excitation) // *Fizika i Tekhnika Poluprovodnikov*, **6**, pp.1936-1944( 1972) (in Russian)
7. V.A. Zuev, V.G. Litovchenko, G.A. Sukach. Mnogochastichnyye rekombinazionnyye processy na poverkhnosti kremniya i germaniya (Many-particle recombination processes at silicon and germanium surfaces) // *Fizika i Tekhnika Poluprovodnikov*, **9**, pp.1641-1648 (1975) (in Russian)
8. W. Michaelis and M.H. Pilkuhn. Radiative recombination in silicon p-n junctions // *Phys.Stat.Sol.*, **36**, p. 311-319 (1969)
9. C.T. Sah. High efficiency silicon solar cells // *Solar Cells* , **17**, p.1 (1986)
10. A.P. Gorban, V.P. Kostilyov, A.V. Sachenko. The optimization of n<sup>+</sup>-p-p<sup>+</sup>-silicon solar cells parameters. Theoretical relations // *Optoelectronika i Poluprovodnikovaya Tekhnika*, No. 34 (1999)
11. M.J. Keevers and M.A. Green. Absorption edge of silicon from solar cell spectral response measurements // *Appl. Phys. Lett.*, **66**, p. 174 (1995)
12. Z.S. Gribnikov, V.I. Mel'nikov. Elektronno-dyrochnoe rasseyaniye v poluprovodnikakh pri vysokikh urovnyakh injekcii (Electron-

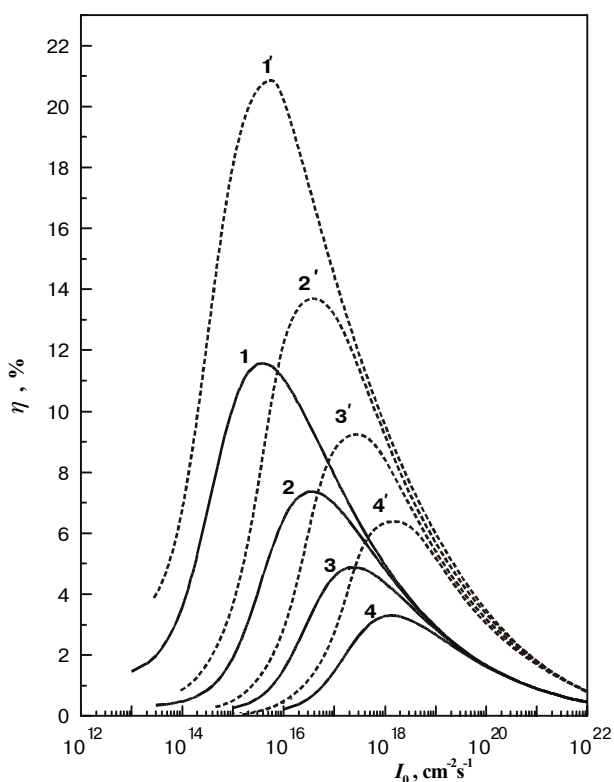


Fig.6. Quantum efficiency of interband radiation as a function of excitation intensity  $I_0$  in the case of many-particle interactions accounted. Parameters used:  $\lambda = 0.5$   $\mu\text{m}$ ,  $d = 100$   $\mu\text{m}$ ,  $s_{0(d)} = 0$ . Shotkey-Reed-Hall life-time  $\tau_r$ , ms: 40 (curves 1 and 1'), 10 (curves 2 and 2'), 3 (curves 3 and 3') and 1 (curves 4 and 4'). Interband radiative recombination constant  $A_i$ , cm<sup>3</sup>/s:  $3 \cdot 10^{-15}$  for curves (1)-(4) and  $6 \cdot 10^{-15}$  for curves (1')-(4')

**A.V. Sachenko, Yu.V. Kryuchenko: Evaluation of the efficiency of interband...**

- hole scattering in semiconductors at high injection levels) // *Fizika i Tekhnika Poluprovodnikov*, **2**, pp.1352-1360 (1968)
13. P.A. Basore. Numerical modeling of textured silicon solar cells / // *IEEE Trans. Electron. Devices*, **37**(2), pp.337-343 (1990)
  14. J. Dzievior and W. Schmid. Auger coefficients for highly doped and highly excited silicon // *Appl. Phys. Lett.*, **31**(5), pp.346-348 (1977)
  15. K. Rajkanan, R. Singh and J. Chewchun. Absorption coefficient of silicon for solar cell // *Solid-State Electron.*, **22**(9), pp.793-796 (1979)
  16. M. Ruff, M. Lindner, U. Rössler, and R. Heilig. The spectral distribution of the intrinsic radiative recombination in silicon // *J. Appl. Phys.*, **74**(1), pp.267-274 (1993)
  17. A. Hangleiter and R. Häcker. Enhancement of band-to-band Auger recombination by electron-hole correlations // *Phys. Rev. Lett.*, **65**(2), pp.215-218 (1990)